
This is an electronic reprint of the original article.
This reprint may differ from the original in pagination and typographic detail.

Haikola, Juha; Tervakangas, Sanna ; Kolehmainen, Jukka; Tittonen, Ilkka

Cathodic arc deposited tetrahedral amorphous carbon as thin film contact pressure sensing material

Published in:
AIP Advances

DOI:
[10.1063/5.0220295](https://doi.org/10.1063/5.0220295)

Published: 01/10/2024

Document Version
Publisher's PDF, also known as Version of record

Published under the following license:
CC BY-NC-ND

Please cite the original version:
Haikola, J., Tervakangas, S., Kolehmainen, J., & Tittonen, I. (2024). Cathodic arc deposited tetrahedral amorphous carbon as thin film contact pressure sensing material. *AIP Advances*, 14(10), 105321 . Article 105321. <https://doi.org/10.1063/5.0220295>

This material is protected by copyright and other intellectual property rights, and duplication or sale of all or part of any of the repository collections is not permitted, except that material may be duplicated by you for your research use or educational purposes in electronic or print form. You must obtain permission for any other use. Electronic or print copies may not be offered, whether for sale or otherwise to anyone who is not an authorised user.

RESEARCH ARTICLE | OCTOBER 16 2024

Cathodic arc deposited tetrahedral amorphous carbon as thin film contact pressure sensing material

Juha Haikola ; Jukka Kolehmainen ; Sanna Tervakangas ; Ilkka Tittonen 



AIP Advances 14, 105321 (2024)

<https://doi.org/10.1063/5.0220295>



Articles You May Be Interested In

In-situ functionalization of tetrahedral amorphous carbon by filtered cathodic arc deposition

AIP Advances (August 2019)

Deposition and properties of tetrahedral amorphous carbon films prepared on magnetic hard disks

J. Vac. Sci. Technol. A (July 2001)

Tunable plasmonic properties of silver nanoparticles embedded in amorphous-carbon ultrathin films deposited by co-sputtering

AIP Conf. Proc. (May 2020)

28 October 2024 12:42:18

AIP Advances

Why Publish With Us?



19 DAYS
average time
to 1st decision



500+ VIEWS
per article (average)



INCLUSIVE
scope

[Learn More](#)

Cathodic arc deposited tetrahedral amorphous carbon as thin film contact pressure sensing material

Cite as: AIP Advances 14, 105321 (2024); doi: 10.1063/5.0220295

Submitted: 31 May 2024 • Accepted: 1 October 2024 •

Published Online: 16 October 2024



View Online



Export Citation



CrossMark

Juha Haikola,^{1,a)}  Jukka Kolehmainen,¹  Sanna Tervakangas,¹  and Ilkka Tittonen² 

AFFILIATIONS

¹Oerlikon Balzers Coating Finland Oy, 02330 Espoo, Finland

²Micro and Quantum Systems (MQS) Group, Department of Electronics and Nanoengineering, Aalto University, 02150 Espoo, Finland

^{a)} Author to whom correspondence should be addressed: juha.haikola@oerlikon.com

ABSTRACT

Tetrahedral amorphous carbon (ta-C) film was deposited using the filtered pulsed cathodic arc deposition method. The ta-C structures deposited on high velocity oxygen fuel thermally sprayed steel beam substrates were investigated for piezoresistive properties under direct contact pressing. A load of up to 1.4 GPa was applied with point contact, with no detrimental influence on the material. The linear response for the strain applied homogeneously on the whole film surface and on the local portion of the film surface under a cylindrical contact was observed. A high gauge factor of the measured system of 305 was measured, showing the potential of the material as a good candidate for sensing applications on direct contact measurement devices.

© 2024 Author(s). All article content, except where otherwise noted, is licensed under a Creative Commons Attribution-NonCommercial-NoDerivs 4.0 International (CC BY-NC-ND) license (<https://creativecommons.org/licenses/by-nc-nd/4.0/>). <https://doi.org/10.1063/5.0220295>

Amorphous carbon thin films show characteristic electrical properties that are similar to those of semiconducting materials.¹ The internal structure and some features are governed by the graphitic and diamond bonds that are sp^2 and sp^3 bonds, respectively, and of their mutual ratio and distribution in the material. A high content of sp^3 bonded carbon gives the material properties similar to those of diamond, resulting in a wide bandgap and insulating properties. However, in amorphous carbon, even a minor sp^2 content generates states within the bandgap, reducing the gap width and adding localized states within the gap, resulting in material with semiconducting properties. In addition, this makes the material sensitive to local structural changes caused, for example, by mechanical strain.² In the present study, the most interesting outcome of this property is that amorphous carbon has been found to exhibit piezoresistivity, with several studies reporting gauge factors in the range from 4 to 80. High gauge factors have been understood to be related to smaller sp^2 cluster size, and with suitable deposition conditions, a-C:H layers have been reported to have even higher gauge factors of up to 1200.^{3,4} Furthermore, there have been additional studies where the structure of amorphous carbon has been modified with an added metal content to enhance the localization of the

conductive clusters to smaller, yet in more numerous, quantities within the non-conductive sp^3 matrix. That is to say, higher gauge factors of up to 3000 have been recorded for the nickel doped a-C structure.⁵

The piezoresistivity of amorphous carbon materials is believed to be influenced by the internal distribution between the sp^2 and sp^3 bonds. That is to say, the distances between the conductive sp^2 clusters embedded into the matrix of electrically insulating sp^3 -bonded structures are affected by the applied strain. It is known that the gauge factor can be increased by increasing the sp^3 bonded carbon content or the distribution of sp^2 clusters, for example, by decreasing their size, in thin films.¹

Amorphous carbon coatings are often used in various tools and components to reduce friction and wear for higher performance and durability.⁶ One can also increase the functionality of the coating by adding an embedded sensing layer for monitoring the tool behavior and thus bringing more added value for the carbon coating, as was already reported.⁷ These smart coatings can typically be used to sense forces that are incident normal to the surface, but planar strains have also been detected. The methods that have been used earlier include ion beam or magnetron sputtering to deposit

amorphous carbon thin films, and measurements with the highest reported gauge factors have been typically conducted by bending, or stretching, the sample. In this work, we apply the pulsed cathodic arc method to deposit tetrahedrally amorphous carbon film and focus especially on the gauge factor and the corresponding electrical response to normal strain.

A set of samples was fabricated on top of 2 mm thick steel substrates, denoted by S235JR. The thin film structures deposited on the substrate were electrically isolated with a thermally sprayed aluminum oxide layer. This sprayed coating was obtained using the high velocity oxygen fuel (HVOF) method. For the thermal sprayed aluminum oxide, typical material properties are assumed as reported in Ref. 8. The deposition of the thin film layers was performed with pulsed cathodic arc process equipment utilizing two sources, described by the patents.^{9,10} During tetrahedral amorphous carbon (ta-C) deposition, 40 SCCM of nitrogen was introduced into the chamber with the purpose of reducing the resistivity of the deposited ta-C carbon material. Samples were rotated during the deposition. A rectangular piezoresistive ta-C thin film layer was deposited at the center of the insulated area having an average measured thickness of 700 nm in the set of many samples. The metallic titanium contact areas were deposited on the edges of the ta-C film, resulting in an 8 mm wide and 4 mm long active area for the ta-C sensing element. Titanium has been reported to form ohmic contact with amorphous carbon thin films, which results in the low contact resistance in the interface.^{11,12} Thus, any influence on the resistance applied by the strain on the titanium–carbon interface is expected to be small.

The ta-C sensing layer was separately deposited on sapphire (aluminum oxide) glass substrates for characterization of basic physical properties. The material mechanical properties, elastic modulus, and hardness were measured by nanoindentation. The elastic modulus measurement resulted in 380.3 ± 16.4 GPa, while the measured hardness was 36.3 ± 1.7 GPa. For the purpose of relating the measured response to the applied normal strain, in addition to the planar strain, the tabulated value for Poisson's ratio, ν , of steel, 0.3, is noted as the main contribution to the planar deformation on thin film structures is assumed to be caused by the changes in the thick substrate plate.

In addition to mechanical characterization, the film was inspected with SEM fracture cross section. The SEM image in Fig. 1 shows a clean smooth structure with occasional larger particles protruding out from the surface.

The sensing element was electrically in contact using conductive epoxy. The resistance of the sensing element was recorded using an Agilent 37942A datalogger 34901A module. The temperature in the vicinity of the measurement device was monitored to exclude the effect of fast changes in temperature on the measured resistance since ta-C material resistivity is known to show a thermistor-like behavior.

The samples were strained using a pusher attached to a computer controlled linear actuator. The actuator was used to push into the system for the maximum length of 0.1 mm, which corresponds to a force of 100 N at maximum. A force sensor was used to measure the force with the datalogger on the ta-C sensing element. Aluminum oxide or silicon nitride was used as a pusher material as the electrically insulating property was required, and the pressure was applied directly to the thin film surface. Three different pushers—a ball, a

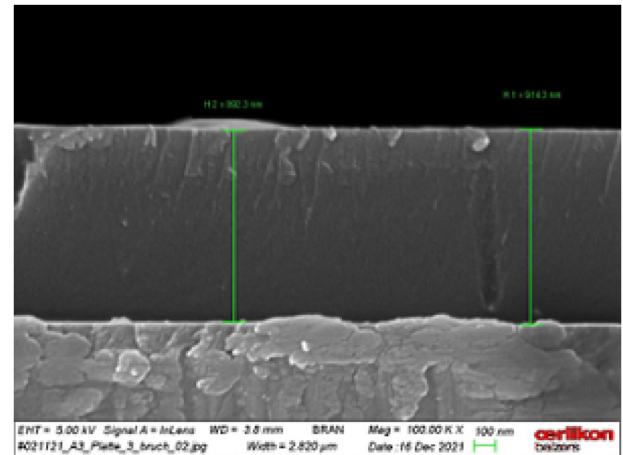


FIG. 1. SEM image illustrating material fracture cross section.

cylinder, and a plate—were used to apply different types of loading on the sample structures.

The actual motion was controlled through pulses, where the load was applied and removed in succession, with the load increasing toward the end of the cycle of the corresponding maximum pusher movement. A single measurement pulse is illustrated in Fig. 2, where the response in the sensing element resistance to the applied force from actual measurement is illustrated. The initial resistance level was roughly 200 kΩ for the sample structures. The change in resistance was interpreted as an average of several cycles as a difference between the initial and excited resistance level before and after the applied load.

The pressure p applied on the samples for each contact type is defined as

$$p = \frac{F}{A} \quad (1)$$

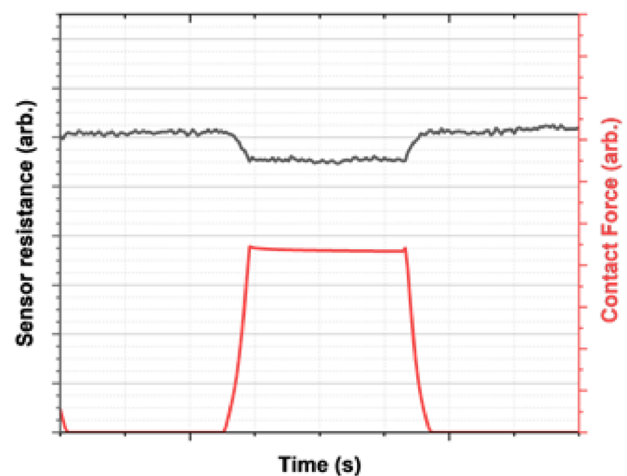


FIG. 2. Typical response of the sensing material resistance in the measurement against the measured applied force.

for the plane contact, where F is the force applied and A is the contact area between the pusher and the sample surface. Correspondingly,

$$p = \frac{2F}{\pi LA} \tag{2}$$

for the line contact, where L is the length of the cylinder in contact with the surface. For the cylinder and plate in contact, the contact area is determined by

$$A = \sqrt{\frac{4FR}{\pi LE^*}} \tag{3}$$

where R is the radius of the cylinder and E^* is the generalized effective modulus,

$$\frac{1}{E^*} = \frac{1 - \nu_1^2}{E_1} + \frac{1 - \nu_2^2}{E_2} \tag{4}$$

Finally, for the point contact,

$$p = \frac{3F}{2\pi A^2} \tag{5}$$

In case of the ball and plate in contact, the contact area is determined by

$$A = \sqrt[3]{\frac{3FR}{2\pi E^*}} \tag{6}$$

where R is now the radius of the ball.

The measurements were conducted with different contact geometries. When using wider contacts, the plunger was set larger than the sensing element area to provide well defined pressure over the element (see Fig. 3), with the main axis of the force aligned with the center of the element. The substrate plate was additionally forced straight by clamps further to the sides of the sample. For the point and line contact, the resistance change is nonlinear against the applied pressure, in correlation to Eqs. (2), (3), (5), and (6). In case of the plane contact, the force and pressure relationship shows a linear behavior, as was also shown in Eq. (1). With non-planar contact, the strain applied on the sensing element is also complex since the deflection of the substrate causes stress and strain in the normal direction and along the surface of the plane in a magnitude larger than that specified by the Poisson ratio of steel.

In the plane contact measurement (see Fig. 4), the strain is readily established by the elastic modulus of the material, and the pressure applied and the gauge factor of the element for the applied normal strain can be calculated as

$$GF = \frac{dR/R_0}{p/E} \tag{7}$$

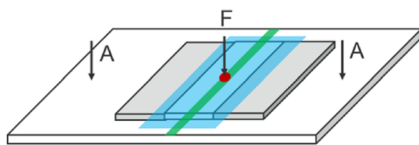


FIG. 3. Schematic diagram showing contacts on the sensing area in the different measurements: plane (blue), line (green), and point (red) contact.

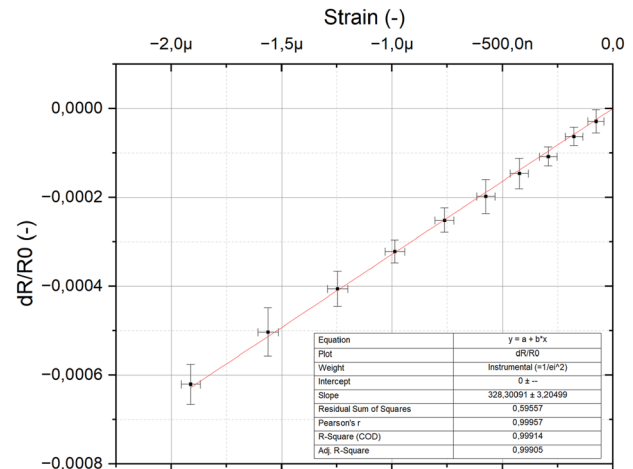


FIG. 4. Measurement curve of relative material resistance change against the contact pressure applied with a planar plunger.

The responses of the studied samples with the applied plane contact are listed in Table I, illustrating the applied pressure and the induced strain on the sample and the measured change in resistance with maximum applied pressure. The gauge factor in each case for the given sample was obtained as the best linear fit on the data.

Finally, we get the result for the average gauge factor of 305 ± 62 , which is based on the measurements of ten samples. The sensitivity to the strain is high when compared to results reported elsewhere from amorphous carbon materials. However, it should be noted that the measurement takes into account neither the contact resistance, which is between the titanium and amorphous carbon thin film layers, nor the changes in the contact resistance as a result of the pressure applied on this area in the case of plane contact measurements. Anyway, we expect titanium and amorphous carbon to

TABLE I. Measurement results for the samples tested in the plate pressing experiment. The force, strain, and resistance change values are obtained at the maximum pressure, whereas the gauge factor is obtained from the linear fit.

Sample	Pressure (MPa)	Strain (10^{-6})	dR/R_0 (10^{-3})	GF
#01	0.72	-1.89	-0.65	305
#02	0.75	-1.97	-0.83	280
#03	0.56	-1.47	-0.64	361
#04	0.7	-1.84	-0.67	321
#05	0.8	-2.11	-0.82	363
#06	0.6	-1.58	-0.54	327
#07	0.57	-1.89	-0.53	254
#08	0.6	-1.50	-0.28	186
#09	0.84	-1.58	-0.4	256
#10	0.72	-2.21	-0.84	358
AVG	305 ± 62

form an ohmic contact with minimal contact resistance even under any change caused by the pressure.

The obtained results are consistent when considering that the coating is a relatively rough thermally sprayed aluminum oxide coating. The measurements display some variation in the established gauge factor between different samples. This is related to the variation between both the film deposited on the rough substrate and the contact formed between the substrate and the plunger used in the measurements. Sometimes the highest applied forces with the point contact measurement caused some damage to the thin film, but this mostly resulted in the change in the base resistance of the specific sample. Thus, the sensing thin film material forms an apparently robust and continuous layer even on the rough substrate.

The elastic modulus of the thin film carbon coating is high compared to the value of 210 GPa of the steel substrate and thermally sprayed layer of 138 GPa.⁸ The pressure applied on the sample causes larger deformation on the rough underlying layers, and the thin top layer also deforms considerably as it conforms to the changes. Thus, the simple model describing strain as the only response at the contact area and pressure applied might not be sufficient to describe the overall strain-resistance relation. On the related matter, it is noted that the strain in the planar direction caused from stretching under pressure was not considered an issue for the purpose of illustrating the high sensitivity of the ta-C film as this would cause an increase in the resistivity of the material as the *sp*² network in the amorphous carbon is pulled apart. Thus, if such an effect takes place, the response to the purely normal strain would be even higher than reported.

The measured resistance change of the element with the line contact is a result of a local resistance change in the proximity of the area of the contact (see Figs. 5 and 6). Since this only affects a small portion of the sensing element surface area, this results in some non-linearity in the measured response. When one considers the contact length in order to obtain simplified approximation of

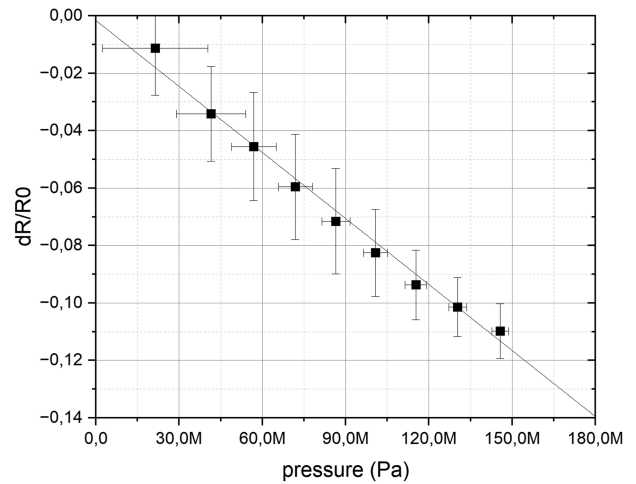


FIG. 6. Relative resistance change of the element corresponding to cylindrical plunger contact width.

the local effect on the resistance change, we obviously again observe a linear response.

The samples were further tested with the point contact for local pressures up to 1.4 GPa (see Fig. 7). The complex local strain response was not, however, obtained, and the linearity, or lack of, was not confirmed on higher pressures. Nevertheless, the resistance response is still smooth with no indication of non-continuities caused by damage to the sample.

This study shows that the studied sample system of thin film tetrahedral amorphous carbon material in contact with the titanium thin film contact layers deposited on the steel substrate isolated with an HVOF thermally sprayed aluminum oxide thick film coating has high sensitivity to strain applied across the thickness of the material. In addition, the overall gauge factor of roughly 300 is linear in the

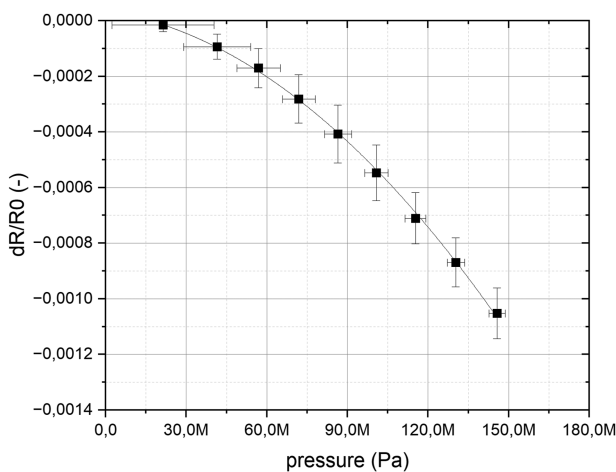


FIG. 5. Measurement curve of relative element resistance change against the contact pressure applied with a cylindrical plunger.

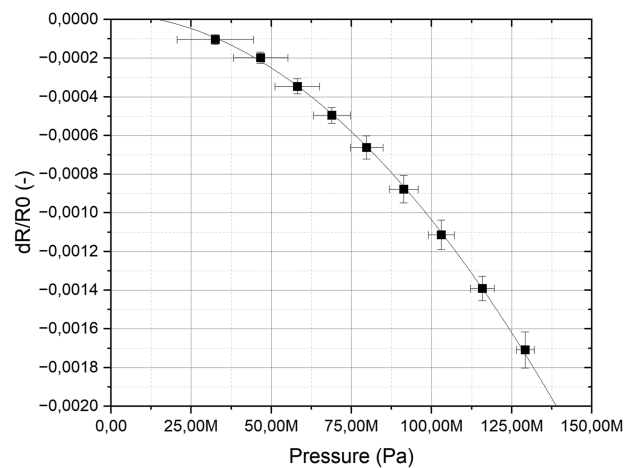


FIG. 7. Measurement of the relative material resistance change against the contact pressure applied with a spherical plunger.

range studied up to the 120 MPa pressure value. With the point contact area, even higher pressures of up to 1.4 GPa were applied, but in this case, the applied strain-resistance relation was not evaluated locally, and the linearity of the relation was not any more established. Ultimately, this study does not distinguish the source of the piezoresistive behavior, and the respective influence of substrate roughness, titanium-carbon interface, and the ta-C films themselves is to be determined.

The material shows a robust behavior in all our tests. We also tested totally unprotected samples, meaning that the thin film was deposited directly on the thermally sprayed aluminum oxide steel substrate. Even in this case, we did not observe any damage or change in the loading tests. The high sp^3 content in the tetrahedral amorphous carbon thin film has a high elastic modulus and hardness, making it very durable.

In addition, the high elastic modulus of the studied thin film material makes it suitable as an integral part in a sensing structure embedded in materials such as metals and ceramics, mainly due to its ability to sustain high loads and its rapid response. Ultimately, the insulating structure such as a thermally sprayed layer needs to be applied on the conductive substrates for proper electrical functionality in a completely embedded sensor structure. Furthermore, the variety of carbon-based thin films could also be utilized as protective layers on the surface of the sensor with the benefit of high integrability on the already carbon-based element.

The authors would like to thank Anssi Metsahonkala, Jarkko Lehti, and Tommi Varis from Tampere University and Thermal Spray Center Finland (TSCF), Tampere, Finland, for their expertise in the manufacture of HVOF sprayed insulating coatings.

AUTHOR DECLARATIONS

Conflict of Interest

The authors have no conflicts to disclose.

Author Contributions

Juha Haikola: Conceptualization (equal); Formal analysis (lead); Investigation (lead); Methodology (lead); Resources (equal); Writing – original draft (lead); Writing – review & editing (equal).

Jukka Kolehmainen: Conceptualization (equal); Supervision (equal); Writing – review & editing (equal). **Sanna Tervakangas:** Conceptualization (equal); Resources (equal); Validation (lead); Writing – review & editing (equal). **Ilkka Tittonen:** Supervision (equal); Writing – review & editing (equal).

DATA AVAILABILITY

The data that support the findings of this study are available within the article.

REFERENCES

- ¹J. Robertson, “Electronic and atomic structure of diamond-like carbon,” *Semicond. Sci. Technol.* **18**, S12–S19 (2003).
- ²A. Tibrewala, E. Peiner, R. Bandorf, S. Biehl, and H. Lüthje, “The piezoresistive effect in diamond-like carbon films,” *J. Micromech. Microeng.* **17**, S77–S82 (2007).
- ³A. Tibrewala, E. Peiner, R. Bandorf, S. Biehl, and H. Lüthje, “Transport and optical properties of amorphous carbon and hydrogenated amorphous carbon films,” *Appl. Surf. Sci.* **252**, 5387–5390 (2006).
- ⁴M. Petersen, R. Bandorf, G. Bräuer, and C. Klages, “Diamond-like carbon films as piezoresistors in highly sensitive force sensors,” *Diamond Relat. Mater.* **26**, 50–54 (2012).
- ⁵S. Meškinis, R. Gudaitis, K. Slapikas, A. Vasiliauskas, A. Ciegis, T. Tamulevičius, M. Andrulevičius, and S. Tamulevičius, “Giant negative piezoresistive effect in diamond-like carbon and diamond-like carbon-based nickel nanocomposite films deposited by reactive magnetron sputtering of Ni target,” *ACS Appl. Mater. Interfaces* **10**, 15778–15785 (2018).
- ⁶B. Schultrich, *Tetrahedrally Bonded Amorphous Carbon Films I: Basics, Structure and Preparation* (Springer, Berlin, Heidelberg, 2018), pp. 195–272.
- ⁷S. Biehl, H. Lüthje, R. Bandorf, and J. Sick, “Multifunctional thin film sensors based on amorphous diamond-like carbon for use in tribological applications,” *Thin Solid Films* **515**, 1171–1175 (2006).
- ⁸G. Bolelli, L. Lusvarghi, T. Varis, E. Turunen, M. Leoni, P. Scardi, C. L. Azanza-Ricardo, and M. Barletta, “Residual stresses in HVOF-sprayed ceramic coatings,” *Surf. Coat. Technol.* **202**, 4810–4819 (2008).
- ⁹J. Kolehmainen, “Focusing unit for an arc discharge apparatus used for plating,” WO1996018754A1, World International Patent Organization, 1996.
- ¹⁰J. Kolehmainen, “Pulsed cathodic arc deposition,” WO2020173598A1, World International Patent Organization, 2020.
- ¹¹F. M. Wang, M. W. Chen, and Q. B. Lai, “Metallic contacts to nitrogen and boron doped diamond-like carbon films,” *Thin Solid Films* **518**, 3332–3336 (2010).
- ¹²A. Zeng, Y. Yin, M. Bilek, and D. McKenzie, “Ohmic contact to nitrogen doped amorphous carbon films,” *Surf. Coat. Technol.* **198**, 202–205 (2005).